reduction has been considered. It involves a system of concentric grids around the interaction region biased in such a fashion that the scattered electrons would travel and be collected at an energy less than required for excitation.

ACKNOWLEDGMENTS

Acknowledgments are due Dr. Edward Soltysik for his work on the earlier definitive portions of the problem, and to Joseph Fabyan for his assistance in the laboratory phase.

PHYSICAL REVIEW VOLUME 133, NUMBER 4A 17 FEBRUARY 1964

Repulsive Interaction Potentials between Rare-Gas Atoms. Heteronuclear Two-Center Systems*

ADOLF A. ABRAHAMSON
The City College of the City University of New York, New York, New York, and Brookhaven National Laboratory, Upton, New York

(Received 30 September 1963)

A theoretical expression, previously applied only to homonuclear pairs of rare-gas atoms, has been used to calculate the interaction energies $U(R)$ for the corresponding heteronuclear two-center systems at internuclear separations R ranging from $0.01a_0$ to $\sim 6.0a_0$ ($a_0=0.529$ Å). These results are compared with: (a) empirical data; (b) other calculations; (c) the geometric-mean rule $U_{AB}=(U_{AA}U_{BB})^{1/2}$; (d) the corresponding united-atom energies. With regard to (a) and (b), this comparison supports conclusions drawn previously from a study of the homonuclear pairwise interactions. That is, the present calculations, too, generally agree more closely with experiment than does either Bohr's screened Coulomb potential or Firsov's Thomas-Fermi type potential. Relation (c) is found to be satisfied, generally, to within a few percent. As for (d), calculations for the He-Ne and Ar-Kr systems indicate that, as $R \to 0$, the electron energy of each system tends, approximately, to the appropriate empirical united-atom value. A similar study of other systems, including the light gases, metals, and certain diatoms, is in progress.

I. INTRODUCTION

A DETAILED knowledge of the interatomic potential $U(R)$ is essential to the solution of a large variety of problems arising in the study of the solid,[1] liquid, and gaseous states.[2–4] At very small interatomic distances $R \lesssim 0.2a_0$ ($a_0=0.529$ Å), Bohr's[5] screened Coulomb potential is a good representation,[6] and at the very much larger near-equilibrium separations, the empirically fitted potentials of the Lennard-Jones (12-6) type (LJ), and of the modified Buckingham (exp-6) type (MB), etc., are applicable.[2] Comparatively little is known concerning $U(R)$, however, in the *intermediate* range of separations, particularly important in the study of phenomena involving close atomic encounters[6–12] or very high pressures and/or temperatures.[13–18] For this reason it seemed worthwhile to examine the reliability of a theoretical expression, U_{TFD}, derived elsewhere[19] on the basis of the Thomas-Fermi-Dirac (TFD) statistical model of the atom[20,21]

* Work supported by the U. S. Atomic Energy Commission.

[1] G. J. Dienes and G. H. Vineyard, *Radiation Effects in Solids* (Interscience Publishers, Inc., New York, 1957), Chap. 2. Also, A. N. Goland, Ann. Rev. Nucl. Sci. **12**, 243 (1962); F. Seitz and J. S. Koehler, in *Solid State Physics*, edited by F. Seitz and D. Turnbull (Academic Press Inc., New York, 1956), Vol. 2, p. 305.

[2] J. O. Hirschfelder, C. F. Curtiss, and R. B. Bird, *Molecular Theory of Gases and Liquids* (John Wiley & Sons, Inc., New York, 1954), Chaps. 1, 3, 12–14.

[3] S. Chapman and T. G. Cowling, *The Mathematical Theory of Non-Uniform Gases* (Cambridge University Press, London, 1960), Chaps. 10–14.

[4] K. E. Grew and T. L. Ibbs, *Thermal Diffusion in Gases* (Cambridge University Press, London, 1952), Chaps. 2, 4, and 5.

[5] N. Bohr, Kgl. Danske Videnskab. Selskab, Mat. Fys. Medd. **18**, No. 8 (1948); see also the first of Ref. 1.

[6] J. B. Gibson, A. N. Goland, M. Milgram, and G. H. Vineyard, Phys. Rev. **120**, 1229 (1960).

[7] D. K. Holmes, in *Radiation Damage in Solids* (International Atomic Energy, Vienna, 1962), Vol. I, p. 12 ff; G. Leibfried and O. S. Oen, J. Appl. Phys. **33**, 2257 (1962).

[8] K. O. Nielsen, in *Electromagnetically Enriched Isotopes and Mass Spectroscopy*, edited by M. L. Smith (Butterworths Scientific Publications, Ltd., London, 1956), pp. 68–81.

[9] O. S. Oen, D. K. Holmes, and M. T. Robinson, J. Appl. Phys. **34**, 302 (1963); M. T. Robinson and O. S. Oen, Appl. Phys. Letters **2**, 30 (1963), and references cited therein.

[10] R. A. Schmitt and R. A. Sharp, Phys. Rev. Letters **1**, 445 (1958).

[11] V. A. J. van Lint and E. M. Wyatt, Jr., U. S. Air Force Report ARL 62-389, 1962 (unpublished), Secs. IX–XI and Appendices VI, IX.

[12] E. A. Mason and J. T. Vanderslice, in *Atomic and Molecular Processes*, edited by D. R. Bates (Academic Press Inc., New York, 1962), p. 663 ff.

[13] I. Amdur, J. Planetary Space Sci. **3**, 228 (1961); see also *Progress in International Research on Thermodynamic and Transport Properties*, edited by J. F. Masi and D. H. Tsai (Academic Press Inc., New York, 1962), Secs. 32, 33, and 49.

[14] I. Amdur and E. A. Mason, Phys. Fluids **1**, 370 (1958).

[15] R. S. Brokaw, second of Refs. 13, p. 271 ff.

[16] P. K. Chakraborti, Indian J. Phys. **35**, 1417 (1961).

[17] T. L. Cottrell, Discussions Faraday Soc. **22**, 10 (1956).

[18] R. E. Walker and A. A. Westenberg, J. Chem. Phys. **31**, 519 (1959); see also R. E. Walker, L. Monchick, A. A. Westenberg, and S. Favin, J. Planetary Space Sci. **3**, 221 (1961).

[19] A. A. Abrahamson, R. D. Hatcher, and G. H. Vineyard, Phys. Rev. **121**, 159 (1961). Hereafter referred to as I.

[20] L. H. Thomas, Proc. Cambridge Phil. Soc. **23**, 542 (1927);

and expected to be approximately valid at these intermediate (as well as smaller) values of R.

For *homo*nuclear pairs of rare-gas atoms, this was done in a previous paper,[22] the pertinent results and notation of which may be summarized here for convenience as follows: The interaction potential of two neutral, ground-state atoms is approximately given by

$$U_{\mathrm{TFD}}(R)=\tfrac{1}{2}(Z_1Z_2e^2/R) \times[\Psi(Z_1^{1/3}R/a)+\Psi(Z_2^{1/3}R/a)]+\bar{\Lambda}, \quad (1.1)$$

where e is the magnitude of the electronic charge; Z_1, Z_2 are the respective atomic numbers of the interacting atoms; Ψ is the TFD screening function[21]; $a=0.8853a_0$; and

$$\bar{\Lambda}=\tfrac{1}{6}\int_{D_{12}}\{\kappa_k[(\rho_{01}+\rho_{02})^{5/3}-(\rho_{01}^{5/3}+\rho_{02}^{5/3})] -2\kappa_a[(\rho_{01}+\rho_{02})^{4/3}-(\rho_{01}^{4/3}+\rho_{02}^{4/3})]\}dv. \quad (1.2)$$

Here $\kappa_k=2.871e^2/a_0$, $\kappa_a=0.7386e^2$; $\rho_{0i}(r_i)$ is the exact, undistorted TFD electron density distribution due to the ith atom, as a function of the radial distance r_i of the volume element dv from the center of this atom ($i=1,2$); D_{12} denotes the overlap region shared by the electron clouds of both atoms 1 and 2. In this approximation, exchange effects are taken into account, but effects of correlation, inhomogeneity (rapid variation of the electrostatic potential near the nucleus), nonvanishing absolute temperatures, and relativity, are neglected. Furthermore, the TFD model of the atom is characterized by a rather unrealistic, sharp cutoff or bounding radius r_b, at which the electron density ρ abruptly drops to zero (see Fig. 1). Despite these shortcomings of the model, however, the theoretical expression (1.1) was found in II to yield potential curves which (a) practically coincide with the Bohr potential at very small separations ($R\lesssim 0.1a_0$–$0.6a_0$) where the latter is generally considered reliable[6]; and (b) are in close or, at least, reasonable agreement with available empirical data at intermediate separations ($R\simeq 0.8a_0$–$7.0a_0$). Over a considerable range of R, with upper limit near $R=r_b$, U_{TFD} was found to be very nearly linear (on a semilogarithmic plot). Calculations based on (1.1) were thus carried up to near $R=r_b$ (typically $\sim 4a_0$), while approximate values of $U(R)$ could be obtained, for about $2a_0$ to $3a_0$ beyond $R=r_b$, by "linear" extrapolation of the calculated curve. Finally, it was shown in II that, apart from comparisons with other theoretical and experimental curves, the validity of U_{TFD} at very small R can also be examined by means of the "united-atom" test,

$$\Delta_{\mathrm{theo}}\equiv\lim_{R\to 0}\{U(R)-(Z_1Z_2e^2/R)\} \to\{H(Z_1+Z_2)-[H(Z_1)+H(Z_2)]\}\equiv\Delta_{\mathrm{exp}}, \quad (1.3)$$

where $H(Z_i)$, $(i=1,2)$, denotes the total electronic ground-state energy (or *total* ionization potential) of an isolated neutral atom of nuclear charge Z_i. In those cases for which the requisite experimental values for the H's in (1.3) are known,[23] application of this test showed that it was satisfied by U_{TFD} with an error not exceeding 20%, or just about that generally associated with the statistical model of the atom *per se*.[24]

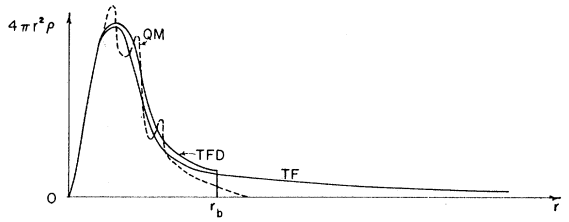

FIG. 1. Electron density distribution in TF and TFD atoms, and quantum-mechanically (QM). (Schematic.)

A priori, these conclusions reached in II could, however, *not* be assumed to hold equally well with regard to *hetero*nuclear systems for the following reasons. Inspection of the basic theoretical relations (1.1), (1.2), and of the united-atom test (1.3), shows that these expressions possess an exceptionally high degree of symmetry when $Z_1=Z_2$, in the sense that then also $\Psi_1=\Psi_2$, where $\Psi_i\equiv\Psi(Z_i^{1/3}R/a)$; $\rho_{01}(r_1)=\rho_{02}(r_2)$ when $r_1=r_2$; and $H(Z_1)=H(Z_2)$. Likewise, $r_{b1}=r_{b2}$, i.e., the artificial bounding radii of atoms 1 and 2, respectively, are equal; and this, in turn, causes also D_{12} in $\bar{\Lambda}$ to be invariably symmetric. As soon as the heteronuclear condition $Z_1\neq Z_2$ is introduced, however, we also have $r_{b1}\neq r_{b2}$; and these two inequalities effectively remove the previous "degeneracies" in that now $\Psi_1\neq\Psi_2$; $\rho_{01}(r_1)\neq\rho_{02}(r_2)$, even when $r_1=r_2$; and also $H(Z_1)\neq H(Z_2)$. The symmetry of D_{12} is likewise destroyed (see Fig. 2). Moreover, the disparity between the atomic radii r_{b1}, r_{b2} (and hence between the "sizes" of the interacting atoms) leads to some entirely new and more involved types of configurations, not encountered under the much simpler conditions envisaged in II (compare Figs. 2 and 15 in II with Figs. 2 and 20 here). Formally, this disparity also renders the evaluation of $\bar{\Lambda}$ somewhat more intricate (see Appendix).

It is the dual purpose of this work, therefore, to determine the reliability of the theoretical relation (1.1) with respect to those heteronuclear pairs of rare-gas atoms for which comparisons with other theoretical and experi-

E. Fermi, Z. Physik **48**, 73 (1928); P. A. M. Dirac, Proc. Cambridge Phil. Soc. **26**, 376 (1930).

[21] P. Gombas, *Die Statistische Theorie des Atoms und Ihre Anwendungen* (Springer-Verlag, Vienna, 1949); P. Gombas, in *Handbuch der Physik*, edited by S. Flügge (Springer-Verlag, Berlin, 1956), Vol. 36.

[22] A. A. Abrahamson, Phys. Rev. **130**, 693 (1963). Hereafter referred to as II.

[23] C. E. Moore, *Atomic Energy Levels*, National Bureau of Standards, Circular No. 467 (U. S. Government Printing Office, Washington 25, D. C., 1949).

[24] O. B. Firsov, Zh. Eksperim. i Teor. Fiz. **33**, 696 (1957) [translation: Soviet Phys.—JETP **6**, 534 (1958)].

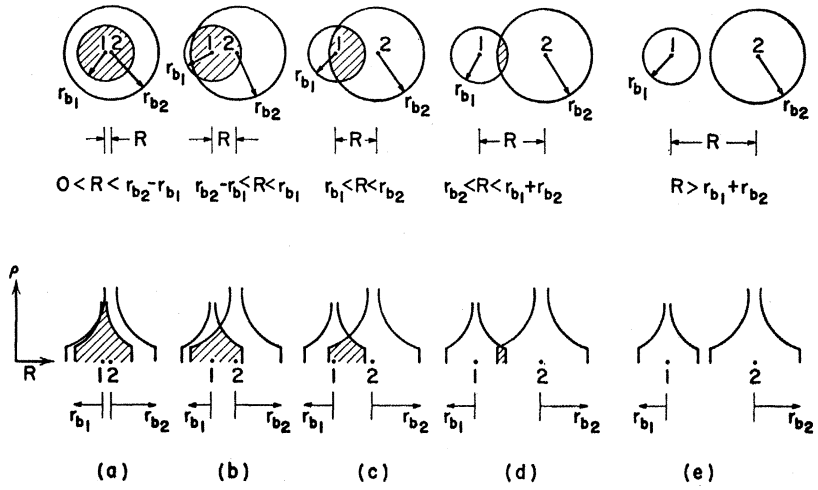

FIG. 2. TFD electron density distribution for a heteronuclear pair of spherically symmetric atoms of radii r_{b1} and r_{b2}, respectively; internuclear separation R, and varying degrees of overlap (shown shaded). (Schematic.)

mental results at very small and intermediate R is possible; and, concomitantly, to present new information concerning $U(R)$ for *all* pairs of unlike rare-gas atoms, in the approximate range of separations $0.01a_0 \leq R \leq 6.0a_0$. Selection of the rare-gas atoms for this purpose was motivated by four main considerations. (1) The theoretical basis of Eq. (1.1) is such that the latter may be expected to hold best for atoms whose electron clouds possess closed-shell configurations,[21] a condition evidently met best by the noble gases; (2) the repulsive interactions between unlike rare-gas atoms are themselves of considerable interest and importance[13–18,25]; (3) knowledge of these interaction potentials can, in turn, be used to calculate those between other, related kinds of atoms,[26] particularly also those involved in the "new" compounds such as Xe-F_4 produced recently by Claassen, Selig, and Malm[27]; (4) by means of the empirical, *geometric-mean* (GM) combining rule,[2,14,28]

$$U_{AB} \simeq (U_{AA}U_{BB})^{1/2}, \tag{1.4}$$

a reliability and internal consistency check may be effected between the results obtained here and those found in II. That is, the extent to which the potential U_{GM}, calculated by means of (1.4) approximates U_{DIR}, the corresponding potential obtained directly via (1.1), may be considered to test the validity of both; for it would seem quite unlikely that *any* two numbers (rather than the appropriate U_{AA}, U_{BB}) would "combine," via (1.4), to yield a given third quantity U_{DIR} computed independently.

In Sec. II, a detailed description of the TFD potentials (1.1), in the light of other theoretical and experimental curves, where available, is given for each heteronuclear pair of rare-gas atoms, exclusive of radon. The order in which these systems are taken up is He-X, (X=Ne, Ar, Kr, Xe); Ne-Y, (Y=Ar, Kr, Xe), etc., through Kr-Xe. A more detailed treatment is given the first of these (He-Ne) in order to provide also a basis for (and avoid repetition in) the discussion of the remaining systems. In Sec. III, the numerical results supporting the TFD curves of Sec. II are tabulated and compared with the corresponding results obtained via (1.4) and the data of II. The potential curves involving radon are given in Sec. IV, and Sec. V summarizes the results and the conclusions reached. The solution of some related computational problems is contained in the Appendix.

II. INTERACTION POTENTIALS NOT INVOLVING RADON

A. Helium-Neon

The He-Ne potentials are shown on a semilogarithmic plot in Fig. 3. Here the TFD curve[29] [Eq. (1.1)] and its dashed extrapolation are compared with two other theoretical curves, namely: (1) Bohr's[5] screened Coulomb potential, U_{B}; and (2) a potential U_{TF}, deduced by Firsov[30] on the basis of the Thomas-Fermi (*not* TFD) statistical model of the atom, in which exchange effects are neglected.[21] At quite small separations, i.e., as R decreases from $\sim 0.5a_0$ to $0.1a_0$, all three theoretical potentials U_{B}, U_{TF}, and U_{TFD} merge, and in view of what has been said about the validity of U_{B} at these values of R, the curves TF and TFD both appear to be fairly reliable here. It will be observed that for R

[25] *Argon, Helium and the Rare Gases*, edited by G. A. Cook (Interscience Publishers, Inc., New York, 1961), especially Vol. I, Chaps. III–IX, and Vol. II, Chaps. XI, XII.

[26] A. A. Frost and J. H. Woodson, J. Am. Chem. Soc. **80**, 2615 (1958).

[27] H. Claassen, H. Selig, and J. Malm, J. Am. Chem. Soc. **84**, 3593 (1962).

[28] I. Amdur, E. A. Mason, and A. L. Harkness, J. Chem. Phys. **22**, 1071 (1954); I. Amdur and E. A. Mason, *ibid.* **25**, 632 (1956); E. A. Mason, *ibid.* **23**, 49 (1955). [The subscripts A, B, in Eq. (1.4) designate two distinct kinds of atoms.]

[29] To maintain continuity and save space, the numerical data supporting the TFD curves shown in this Section are collected in Table III of Sec. III.

[30] O. B. Firsov, Zh. Eksperim. i Teor. Fiz. **32**, 1464 (1957) [translation: Soviet Phys.—JETP **5**, 1192 (1957)], and Ref. 24.

larger than $\sim 0.5a_0$, U_B appears to fall off far too steeply with increasing R. Indeed, at $R=4a_0$, U_B is too small by more than one order of magnitude. Conversely, U_{TF} is seen to decrease too slowly with increasing R, remaining roughly as much above U_{emp} as U_B stays below. This behavior[31] of U_B and U_{TF} is thus entirely analogous to that observed in II. There, the much too slow decrease of U_{TF} was shown to be a consequence of the unrealistically expansive electron cloud of the TF atoms.

The remaining three potentials[14,32] shown in Fig. 3 are empirical ones, U_{emp}, and hence, comparison of the TFD curve with them is of especial interest. It must be remembered, however, that just because these are empirical potentials, their reliability is restricted, approximately, to the interval of separations S_{emp}, defined by $R_l \leq R \leq R_u$, in which the corresponding measurements were made. (Here R_l and R_u, respectively, denote the lower and upper limits on R.) At separations R lying progressively further and further outside these limits, comparison of U_{TFD} with extrapolations of these U_{emp} is, therefore, of progressively less certain significance. Table I gives the approximate values of R_l and R_u, and it is readily seen that while R_u is generally sufficiently large to permit comparison of *un*extrapolated U_{emp} with U_{TFD} at "large" R, the values of R_l often are so large that these unextrapolated U_{emp}, unfortunately, cannot serve as dependable criteria for the validity of U_{TFD} at separations much smaller than $3a_0$ to $6a_0$.

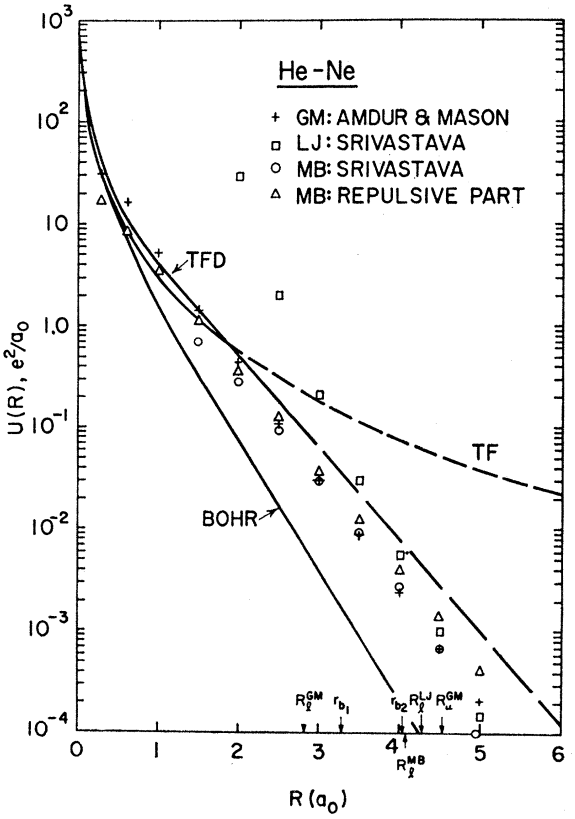

FIG. 3. Repulsive interaction potentials for the He-Ne system.

[31] This has also been noted previously by other workers, e.g., those of Ref. 6.

[32] K. P. Srivastava, J. Chem. Phys. 28, 543 (1958).

TABLE I. Approximate lower and upper limits, R_l and R_u, of ranges of separations over which some of the potentials shown in Figs. 3–19 were fitted empirically. (Atomic units.)[a]

System	R_l	R_u	Type	Reference
He-Ne	2.85	4.54	GM	14
	4.3	···	LJ	32
	4.1	···	MB	32
He-Ar	3.40	5.29	GM	14
	4.95	···	LJ	32
	4.76	···	MB	32
	3.10	4.28	AX	40
	4.18	4.86	WW	41
He-Kr	3.2	5.3	GM	14
	5.3	···	LJ	32
	5.1	···	MB	32
He-Xe	3.42	5.43	GM	14
	5.48	5.75	LJ	32
	5.3	5.7	MB	32
Ne-Ar	3.74	5.37	GM	14
	5.2	···	LJ, MB	32
	3.6	4.6	AX	42
Ne-Kr	3.9	5.5	GM	14
	5.6	···	LJ, MB	32
Ne-Xe	4.3	5.7	GM	14
	5.7	···	LJ, MB	32
Ne-Rn	5.65	···	LJ	43
	5.4	···	MB	43
Ar-Kr	4.35	6.52	GM	14
	6.3	···	LJ, MB	32
Ar-Xe	4.8	6.8	GM	14
	6.4	···	LJ, MB	32
Ar-Rn	6.2	···	LJ, MB	43
Kr-Xe	5.1	6.9	GM	14
	6.7	···	LJ, MB	32
Kr-Rn	6.3	···	LJ, MB	43

[a] No entry is shown where R_u is not given in, or is not readily calculable from, the corresponding reference.

Keeping these points in mind, one is led to the following conclusions concerning U_{TFD} for the He-Ne interaction. In the range of "large" separations $4a_0 \lesssim R \lesssim 5a_0$, in which the LJ and MB potentials *are* valid (Table I), the extrapolated TFD curve exceeds the latter by a factor ranging approximately from 2 to 10, the discrepancy generally increasing with R. Poor agreement at these separations is not unexpected,[19,22] and it may be of interest to specify some of its probable causes. Perhaps the most obvious of these is the crudeness of our extrapolation procedure, i.e., of simply extending the calculated nearly-linear portion of U_{TFD}.

Secondly, it is clear from Fig. 2 that, as R increases from very small values towards $R=r_{b1}$ (chosen to be $<r_{b2}$ always), the unrealistic behavior of the electron-density distribution near the cutoff radius $r_i=r_{bi}$ $(i=1,2)$ plays a progressively more and more significant role in the evaluation of the two-center integral $\bar{\Lambda}$ over the overlap region D_{12} [Eq. (1.2)]. Even at separations *approaching* r_{b1}, therefore, the reliability of U_{TFD} may be expected to decrease. Thirdly, other things being equal, the *statistical* nature of the TFD approximation naturally tends to render results based on it intrinsically the less reliable, the smaller the number of electrons involved; or, in the case of neutral atoms considered here, the smaller the sum (Z_1+Z_2), i.e., the lighter the pair of interacting atoms. Consequently, of all the TFD curves under consideration in this work, that for the He-Ne system with a total of merely 12 electrons might be expected to be one of the least accurate at large R. Comparison of Fig. 3 with those for each of the remaining systems indeed substantiates this conclusion. Finally, the correlation correction U^c as well as the (Weizsäcker) inhomogeneity correction U^i are both known to be important mainly for interactions involving the *edge* $(r\simeq r_{bi})$ of one or more atoms, and to be negative in sign in that case.[21,33,34] Neglecting both U^c and U^i, as we have done here, would therefore also tend to render U_{TFD} unduly large as $R\rightarrow r_{b1}$, likewise in agreement with observation.[35]

In addition to the probable causes listed in the preceding paragraph, it should be pointed out that, for reasons not clear to the writer, *all* TFD curves involving neon deviate significantly more strongly from U_{MB} near $R\sim 5a_0$ than do the curves *not* involving neon. This fact is illustrated also in Table II.

"Inward" extrapolations of the U_{emp} to values of R less than R_l are thus plotted here and in the succeeding graphs not to serve as "experimental" criteria by which the validity of the theoretical TFD curve can be reliably tested, but rather for the following reasons. It was pointed out by Amdur,[13] and specifically confirmed in II wherever comparison with experiment was possible, that U_{LJ} rises unduly rapidly as R decreases below R_l, so that the extrapolated U_{LJ} generally exceeds the values of other U_{emp} at these separations by orders of magnitude. Thus,

$$U_{\mathrm{emp}}\ll U_{\mathrm{LJ}} \quad \text{when} \quad R<R_l. \tag{2.1}$$

With regard to U_{MB}, on the other hand, it was found that for the systems examined in II,

$$U_{\mathrm{emp}}\gtrsim U_{\mathrm{MB}} \quad \text{when} \quad R_{\max}<R<R_l, \tag{2.2}$$

with U_{MB} generally staying *within* an order of magnitude of U_{emp}, and often much closer. Now, it is well known[2] that when R becomes sufficiently small, U_{MB} goes through a spurious maximum at $R=R_{\max}$, and thence falls off rapidly to $-\infty$. For $R<R_{\max}$, U_{MB} is therefore not usable. It was further noted in II, however, that if only the *repulsive* part U_{rep} (rather than the total U_{MB}) is considered, reasonable agreement with available experimental data continued down to separations considerably less than $R_{\max}$ and, *a fortiori*, less than R_l^{MB}. That is,

$$U_{\mathrm{emp}}\sim U_{\mathrm{rep}},$$
$$\text{when} \quad (R_{\max}-1a_0)\lesssim R\lesssim (R_{\max}+1a_0)<R_l^{\mathrm{MB}}. \tag{2.3}$$

At first sight, consideration of U_{rep} separated from the attractive term of U_{MB} may seem arbitrary, and the agreement therefore fortuitous. Actually, however, this procedure would appear to be quite consistent with Buckingham's observation[36] that in the potential bearing his name, the attractive term "has little real significance inside the zero of the potential and its retention there tends to obscure the nature of the rise of the potential at smaller distances. For this reason, some empirical potentials in use effectively eliminate this negative term for small R." [The question whether or not the observed relation (2.3) is, nevertheless, merely accidental will not be further pursued here.]

We now note that, in view of (2.1) and (2.2), it is necessary that an acceptable theoretical potential function U_{theo} satisfy the relation

$$U_{\mathrm{MB}}<U_{\mathrm{theo}}\ll U_{\mathrm{LJ}} \quad \text{when} \quad R_{\max}<R<R_l. \tag{2.4}$$

This, of course, is not a sufficient condition on U_{theo}, since the latitude allowed U_{theo} by (2.4), especially at small R, extends over several orders of magnitude.[37] From Fig. 3 we see that U_{TFD} does satisfy conditions (2.3) approximately, and (2.4) exactly. In view of the preceding remarks, it is evident that this does *not*

TABLE II. Approximate values of the ratios $U_{\mathrm{TFD}}/U_{\mathrm{MB}}$, and of their averages, at three separations R near R_l^{MB}.

Neon present					Neon absent				
System	$R(a_0)$	4.5	5.0	5.5	System	$R(a_0)$	4.5	5.0	5.5
Ne-He		4	10	···	He-Ar		1.1	1.5	2.7
Ne-Ar		2.4	3.0	···	He-Kr		1.1	1.1	1.5
Ne-Kr		2.3	2.6	3.6	He-Xe		1.0	1.0	1.3
Ne-Xe		2.0	2.3	2.8	Ar-Kr		1.0	1.0	1.0
Ne-Rn		4.1	3.8	4.5	Ar-Xe		1.0	1.0	1.1
					Ar-Rn		2.0	1.6	1.4
					Kr-Xe		1.5	1.2	1.1
					Kr-Rn		2.3	2.0	1.8
Average		3.0	4.3	3.6	Average		1.4	1.4	1.5

[33] Y. Tomishima, Progr. Theoret. Phys. (Kyoto) **22**, 1 (1959).
[34] J. M. Keller, thesis, Xavier University, 1959 (unpublished); see also Refs. 46 and 47, below.
[35] Preliminary studies of U_{TFD} for metals, too, tend to confirm this conclusion.
[36] R. A. Buckingham, Trans. Faraday Soc. **54**, 453 (1958).
[37] Reliable experimental data at these small $R<R_l$ would clearly be much preferable for checking the validity of U_{theo} (e.g., U_{TFD}). Unfortunately, as far as the writer could ascertain, however, such data are presently available for only very few systems (see below), and even there over only a very restricted range of R. [Indeed, it was partly this very paucity of available information on $U(R)$ which gave added impetus to this investigation.]

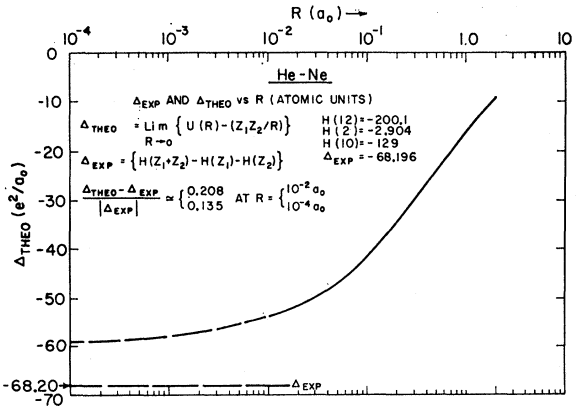

FIG. 4. United-atom test for the He-Ne potential.

constitute reliable experimental verification of U_{TFD}. It does mean, however, that if past experience,[22] and relations (2.3) and (2.4) may be used as rough guides, then in the interval $0.3a_0 \leq R \leq 3.0a_0$, U_{TFD} is likely to be in error by not more than an order of magnitude, possibly by very much less. In any event, in the absence of reliable empirical data at these separations, a more definite appraisal of our theoretical potential there would presently not appear possible.

Lastly, concerning Fig. 3, the points due to Amdur and Mason[14] (GM) are obtained semiempirically, i.e., by application of the GM rule (1.4) to the results of their He-He and Ne-Ne scattering experiments.[38] Inasmuch as these values U_{GM} practically coincide with those of U_{MB} already discussed, little concerning the former need be added here. It will be observed, however, that this near-coincidence again tends to confirm relation (2.2).

We conclude our consideration of the He-Ne system by noting that the united-atom test [Eq. (1.3)] is satisfied by U_{TFD} here to within $\sim 21\%$ at $R=0.01a_0$, and to within $\sim 14\%$ at $R=10^{-4}a_0$ (Fig. 4). The latter value of R, of course, constitutes a better realization of the condition $R \rightarrow 0$ of the test (1.3), and the correspondingly smaller error of 14% lies well within that of 20% generally associated with the statistical model.[24]

The united-atom test, unfortunately, can here be applied to only this system and to Ar-Kr (see Fig. 12, below), because for all other pairs in this group, the required experimental values for total ionization potentials H in (1.3) are presently unknown.

B. Helium-Argon

For the He-Ar interaction (Fig. 5), a somewhat more extensive comparison of U_{TFD} with experiment is possible. At $R \simeq 5a_0$, where the U_{emp} *are* valid (Table I), U_{MB} and U_{LJ} are seen just to "bracket" the extrapolated TFD curve between them.[32,39] This state of affairs persists through most of the remaining systems, and contrasts sharply with the discrepancy, by a factor of ~ 10, between U_{emp} and U_{TFD} at $R \simeq 5a_0$, for the He-Ne system (Fig. 3). Since the extrapolation procedure employed is the same throughout, and since the change in the numerical values of r_{b1}, r_{b2} is small, the much improved agreement between U_{emp} and U_{TFD} near $R=5a_0$ in the present and most of the following cases suggests that it may have been largely the relative paucity of electrons in the He-Ne case which was responsible for the much larger discrepancy observed there (but see also fourth paragraph of Sec. II A above).

In the region $3a_0 \lesssim R \lesssim 5a_0$, two slightly overlapping experimental segments of $U(R)$ are available for comparison with the TFD curve [Eq. (1.1)]. The first of these, due to Amdur *et al.*[40] (AX), is valid from $\sim 3.1a_0$ to $4.3a_0$. The other (WW), due to Walker and Westenberg,[41] applies to separations ranging from $\sim 4.2a_0$ to $4.9a_0$. It will be noted that the *maximum* relative difference of $\sim 25\%$ between the TFD curve and these empirical segments is comparable to that between the experimental results themselves (where these overlap). As observed both in II and in the He-Ne

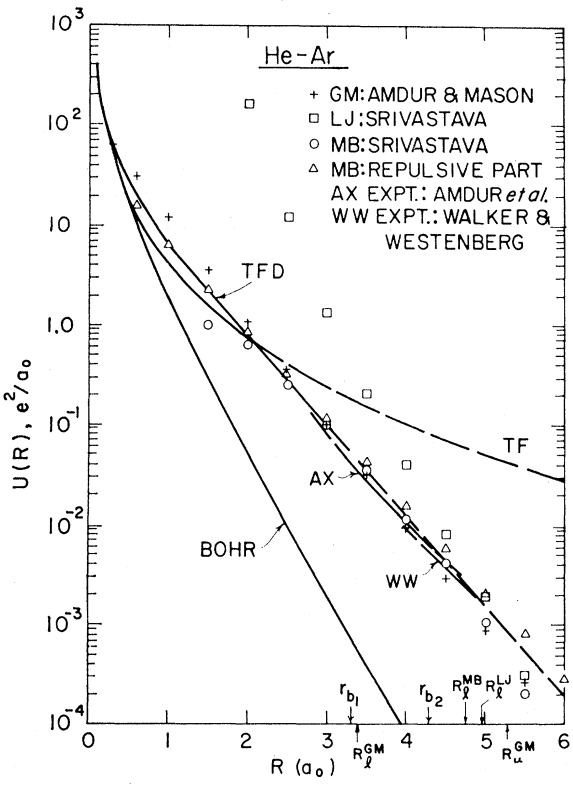

FIG. 5. Repulsive interaction potentials for the He-Ar system.

[38] I. Amdur and A. L. Harkness, J. Chem. Phys. **22**, 664 (1954). E. A. Mason and J. T. Vanderslice, Ind. Eng. Chem. **50**, 1033 (1958); see also Ref. 14.

[39] E. A. Mason and W. E. Rice, J. Chem. Phys. **22**, 522, 843 (1954).

[40] See the first of Refs. 28.

[41] See the first of Refs. 18.

system (Fig. 3) above, both U_B and U_{TF} differ also here (Fig. 5) markedly from the experimental curves at these separations, generally by orders of magnitude. Similar remarks apply to U_{LJ} when $R \ll R_l$, likewise noted already in both II and the He-Ne interaction (Fig. 3).

Another feature, also noted in II, is the close agreement between U_{MB} and U_{TFD} even when the former is extrapolated to separations R far below R_l^{MB}, here to $\sim 2a_0$. For internuclear distances smaller than this, U_{MB} is seen to arc over towards its usual, spurious maximum so that *there* U_{MB} becomes totally unrealistic. Its *repulsive* part U_{rep} alone, however, is seen to agree with U_{TFD} fairly closely from $\sim 4a_0$ down to $\sim 1a_0$. (For $R \lesssim 0.5a_0$, U_{rep} must be cut off, of course, because its negative-exponential form unrealistically gives $U_{rep} \to$ constant as $R \to 0$.) In view of the large extrapolations involved, none of the statements in this paragraph should be construed as reliable experimental support for the accuracy of the TFD potential in this range. One wonders, nevertheless, whether those statements may not be significant after all,[22] especially in the light of (1) the fairly reasonable agreement, at $R \ll R_l$, of U_{MB} and/or U_{rep} with the experimental curves where such are available (AX and WW here; Ne-Ar, Fig. 8 below; and Figs. 4, 6, 7, 11 of II); (2) Buckingham's remark[36] concerning U_{rep}, cited in Sec. II A.

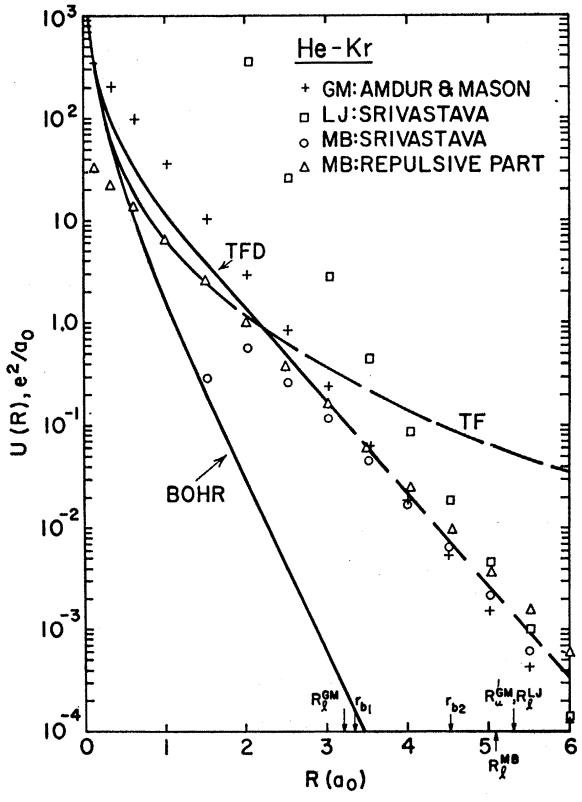

FIG. 6. Repulsive interaction potentials for the He-Kr system.

In the interval $3.5a_0 \lesssim R \lesssim 5.0a_0$ within which U_{GM} is applicable (Table I), the latter[14] can be seen to be approximated quite closely by U_{TFD} near the lower limit of this interval. As the upper limit is approached, U_{TFD} falls off more slowly than U_{GM} until at $R = 5a_0$, $U_{TFD} \approx 2U_{GM}$. The significance of this disagreement of U_{TFD} with U_{GM} should be viewed with some reservation, however, because U_{GM} itself is seen to diasgree in similar manner with the *experimental* segments AX and WW in this interval.

At very small separations $R \lesssim 0.3a_0$, U_B, U_{TF}, and U_{TFD} are seen practically to coalesce in much the same way as found in both II and Fig. 3.

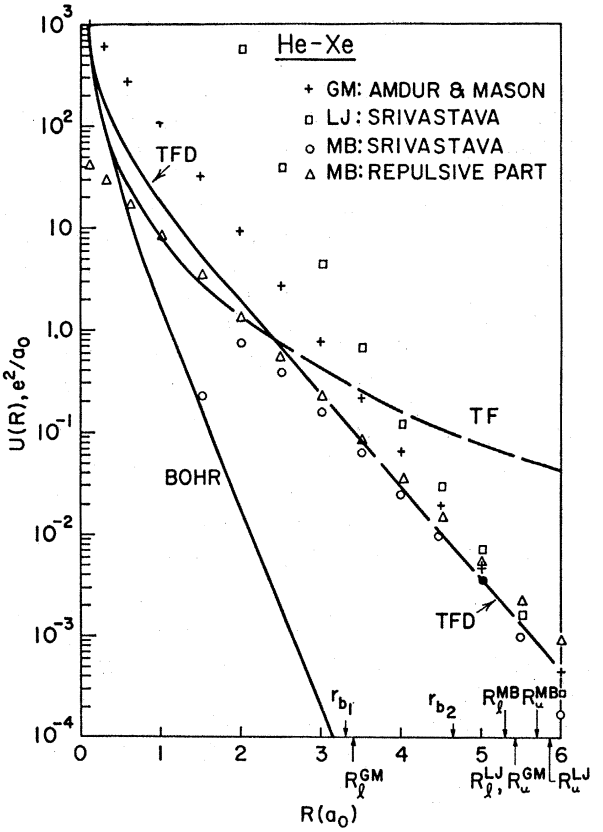

FIG. 7. Repulsive interaction potentials for the He-Xe system.

C. Helium-Krypton

For this system (Fig. 6), $R_l^{MB,LJ} \sim 5a_0$, at which separation the extrapolated TFD potential is just slightly higher than U_{MB}.[32] At $R = 5.5a_0$, $U_{TFD} \simeq U_{LJ} > U_{MB}$ (and the inequality here may be an indication of the uncertainty in each of these U_{emp}). At $R = 6.0a_0$, U_{TFD} appears to be definitely too large, at least by a factor of ~ 2. At $R < R_l^{MB}$, U_{TFD} follows U_{rep} down to $R \sim 3a_0$ (whereas, with decreasing R, U_{MB} is plainly seen to "bend over" towards its spurious maximum, and thence to $-\infty$). Agreement of U_{TFD} with this extrapolation of U_{rep} to such small R can, of

course, not be construed as reliable experimental verification of U_{TFD} there, but may be worth noting in the sense described previously (Sec. II B).

In their range of validity, $3.2a_0 \lesssim R \lesssim 5.3a_0$ (Table I), the semiempirical GM values[14] are seen to be approximated by U_{TFD} to within a factor of ~ 2, often much more closely. Again, the "spread" between the GM, LJ, and MB values at a given R may be a rough indication of the uncertainty in each.

Here, too, U_{LJ} shows its typical, very rapid rise with decreasing R, and also U_{B} and U_{TF} display their by now familiar[22] behavior of, respectively, falling off too rapidly and too slowly with increasing R. Likewise as

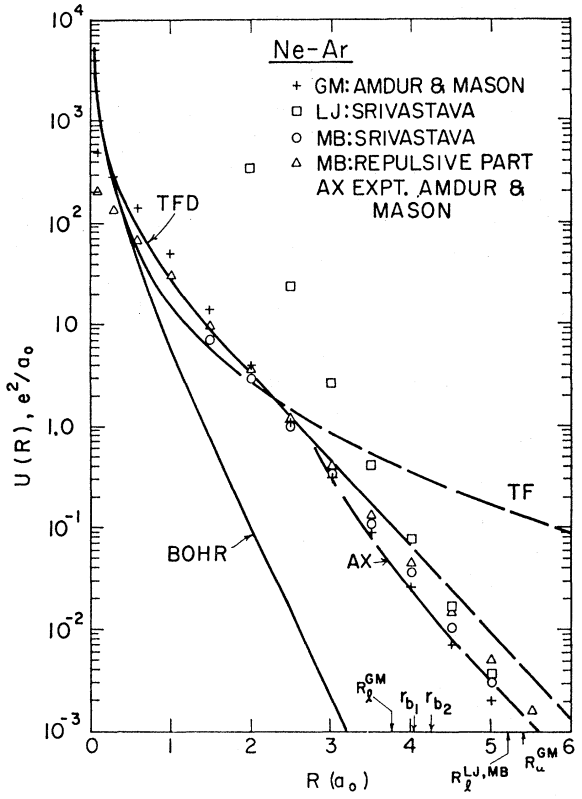

FIG. 8. Repulsive interaction potentials for the Ne-Ar system.

found before, U_{B} and U_{TF} merge at $R \lesssim 0.5a_0$, and both coalesce with U_{TFD} when $R \lesssim 0.2a_0$.

D. Helium-Xenon

The same types of potential[14,32] as shown previously are plotted for the He-Xe system in Fig. 7. Inasmuch as the behavior of U_{TFD} compared to the other potentials is quite similar to that described in detail in the preceding cases, no further comment is necessary here.

E. Neon-Argon

In the light of the preceding graphs and their discussion, the various Ne-Ar potentials[14,32,42] shown in Fig. 8

[42] See the second of Refs. 28.

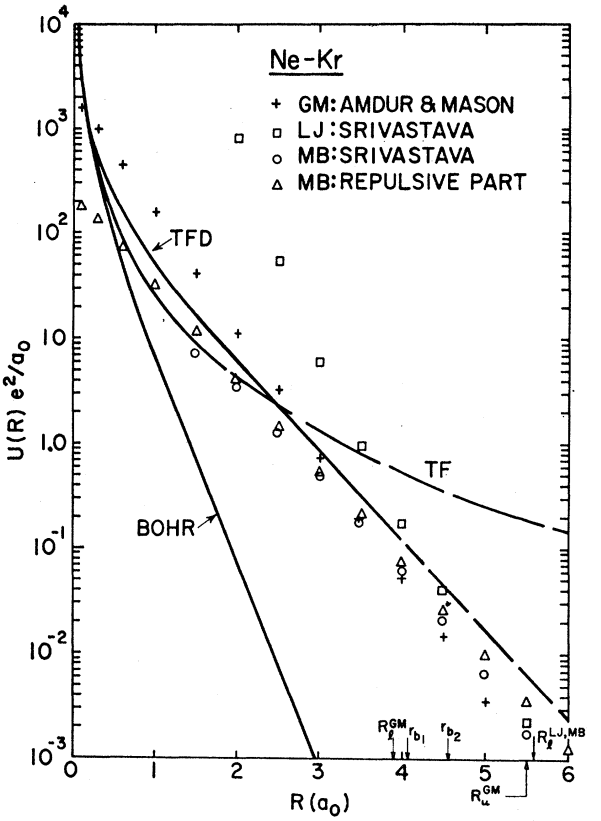

FIG. 9. Repulsive interaction potentials for the Ne-Kr system.

are fairly typical and self-explanatory. As far as comparison with empirical values is possible, the disagreement between the latter and U_{TFD} here would seem somewhat worse than in most of the preceding cases. At large $R \sim 4$–$5a_0$, this feature is found to recur also in the remaining interactions involving neon, a characteristic behavior already commented on in conjunction with the discussion of the He-Ne system (Fig. 3 and Table II). Beyond this and the more general weaknesses of the expression (1.1) discussed earlier, no simple explanation for this state of affairs is apparent to the writer.

F. Neon-Krypton

Figure 9 shows the Ne-Kr potentials. Whatever little empirical data[14,32] are available for comparison here (chiefly for $R > 4a_0$), these suggest that (as in the preceding case) U_{TFD} is too large, at least for $4a_0 < R \leq 5.5a_0$, by a factor (increasing with R) ranging from about 2 to 5. See also Sec. II E.

G. Neon-Xenon

The Ne-Xe interactions are depicted in Fig. 10. The theoretical curves U_{B}, U_{TF}, again show their typical course relative to U_{TFD}, as do[14,32] the U_{emp} and their extrapolations. A feature of some interest here is the

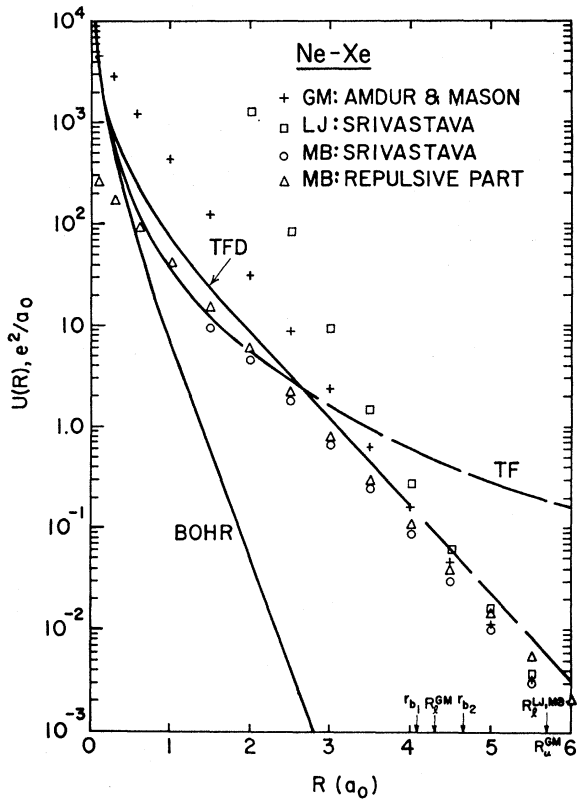

FIG. 10. Repulsive interaction potentials for the Ne-Xe system.

gradual confluence, with decreasing R, of the semi-empirical $U_{\rm GM}$ with $U_{\rm TFD}$ until, at $R\approx R_l^{\rm MB}\simeq 4.0a_0$, agreement between these two potentials is practically complete. See also Sec. II E.

H. Argon-Krypton

In addition to some features familiar by now, Fig. 11 for the Ar-Kr interaction[14,32] also shows certain novel ones. The most striking of these is the practically complete agreement of $U_{\rm TFD}$ with the extrapolated $U_{\rm MB}$ from $R=5.5a_0$ down to near $3.5a_0$; and with $U_{\rm rep}$, approximately, even further. Again, because of the extrapolations involved, this accord is, of course, significant only in the restricted sense already described in Secs. II A and C. Similar to the Ne-Xe interaction (Fig. 10), we note that also here $U_{\rm GM}$ approaches $U_{\rm TFD}$ closely as R decreases towards $R_l^{\rm GM}\sim 4.0a_0$.

The TFD potentials for systems involving argon form a counterpart to those involving neon, in the following sense. Whereas the latter potentials agree worst of all with $U_{\rm emp}$ at large $R(\sim 4.5$ to $5.5a_0)$, just the opposite holds for the TFD curves involving argon. This latter fact is borne out by Figs. 5 above and 11 here, as well as by Figs. 13 and 17 below. As in the case of the exceptionally poor agreement in the Ne-X type systems, so also is there no obvious reason apparent to the writer for explaining this "good" accord found in the Ar-X type systems.

The united-atom test (1.3), applied to Ar-Kr, is described in Fig. 12. At $r=0.01a_0$, the test shows a large relative error (39%) in $\Delta_{\rm theo}$. Extrapolating $\Delta_{\rm theo}(R)$ to $R=10^{-4}a_0$, and thereby fulfilling the condition $R\to 0$ much better, however, reduces the relative error in $\Delta_{\rm theo}$ to $\sim 19\%$. This is within the accuracy of $\sim 20\%$ generally ascribed to the statistical model.[24]

I. Argon-Xenon

The general features of this interaction[14,32] (Fig. 13) are so similar to those of the preceding system that further comments here are superfluous.

J. Krypton-Xenon

For the Kr-Xe system (Fig. 14), $R_l^{\rm GM}\simeq 5a_0$, and it is seen[14] that the ratio $U_{\rm TFD}:U_{\rm GM}\sim 1:2$ to $1:4$ for $5a_0\leq R\leq 6a_0$. The agreement of $U_{\rm TFD}$ with[32] $U_{\rm MB}$ (and with $U_{\rm rep}$), though considerably closer, may be of but limited significance, however, because of the extrapolations involved (See Secs. II A and C).

III. NUMERICAL RESULTS AND THEIR ANALYSIS

In Table III, the numerical values of $U_{\rm TFD}$ for systems not involving radon are given (a) as found by

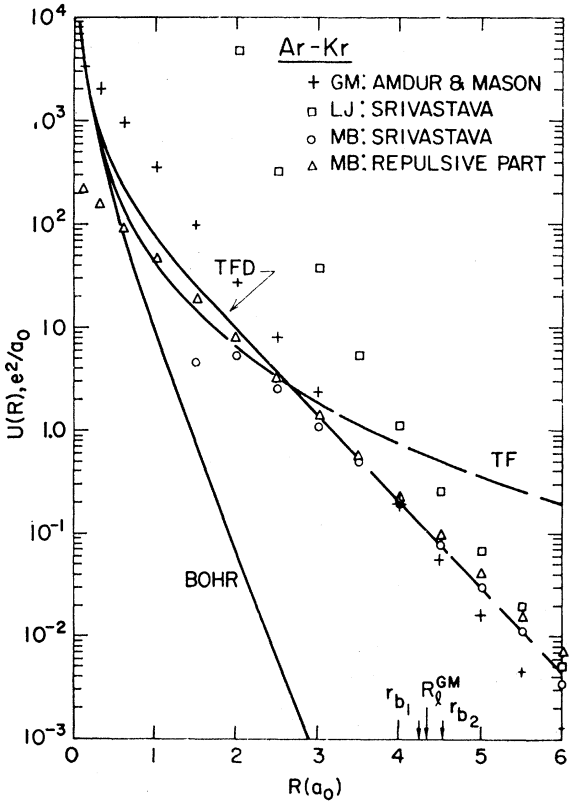

FIG. 11. Repulsive interaction potentials for the Ar-Kr system.

direct calculation using Eq. (1.1); and (b) by application of the GM rule (1.4) to the results of II. In both cases, the calculations are carried up to the value of R nearest to $r_{b1}(<r_{b2})$. For $R>r_{b1}$, extrapolated values of $U(R)$, read off the graphs to two significant figures only, are tabulated with distinguishing superscript a. Inspection of Table III shows the agreement between these two sets of numerical results (U_{DIR} and U_{GM}) to be generally quite close. In order to give a clearer and more precise account of the extent of this accord, numerical values of

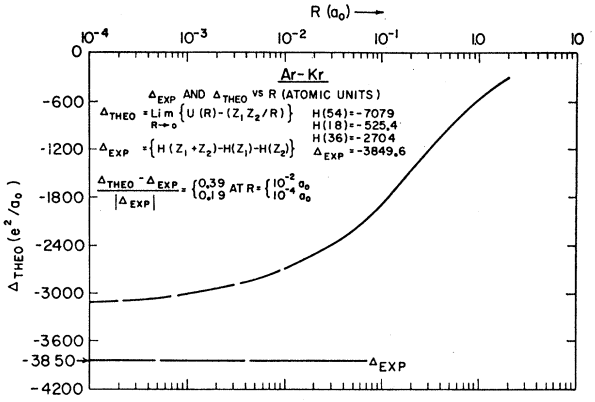

FIG. 12. United-atom test for the Ar-Kr system.

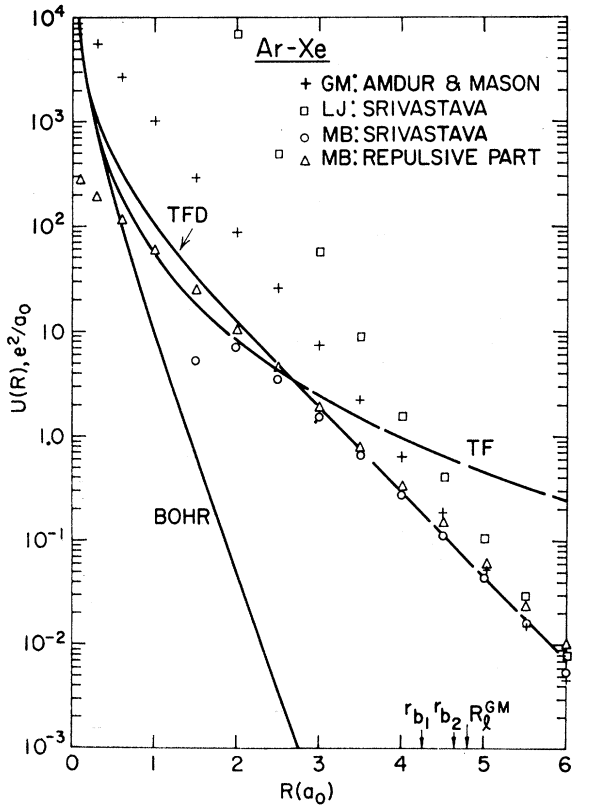

FIG. 13. Repulsive interaction potentials for the Ar-Xe system.

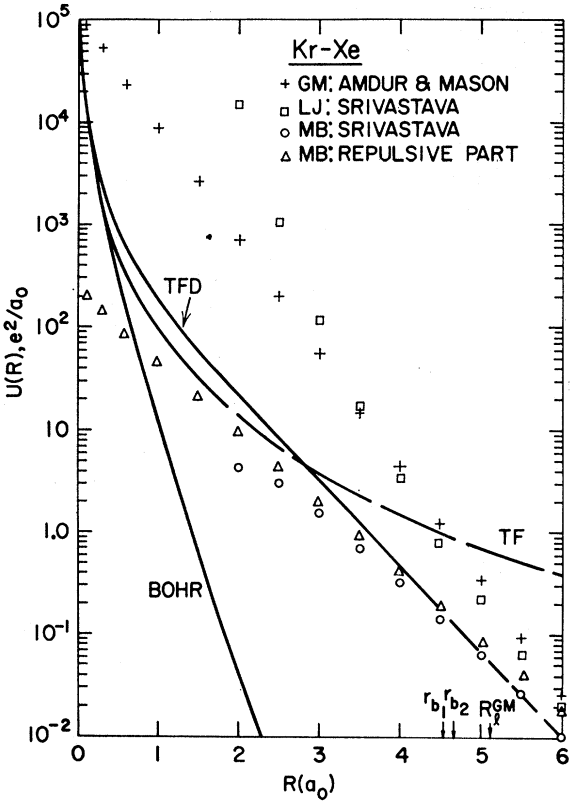

FIG. 14. Repulsive interaction potentials for the Kr-Xe system.

the relative differences, A, between U_{GM} and U_{DIR}, i.e.,

$$A\equiv(U_{\mathrm{GM}}-U_{\mathrm{DIR}})/U_{\mathrm{DIR}} \tag{3.1}$$

have been recorded in Table IV. From there is it seen that A is predominantly negative; ranges (in magnitude) mostly from $\sim 0.1\%$ (or less) to $\lesssim 10\%$; and exceeds the latter value in but one isolated instance (He-Xe at $R=1.5a_0$). To within this accuracy, the GM rule is, therefore, evidently satisfied.

This generally close agreement between U_{DIR} and U_{GM} may be regarded as a measure of the accuracy of the "unknowns" U_{AA}, U_{BB}, and $U_{AB}{}^{\mathrm{DIR}}$ (in obvious notation) entering into (3.1). That is, ideally we should have

$$|A|=0, \tag{3.2}$$

and as we have just seen (Table IV), $|A|$, indeed, mostly approximates this condition quite closely (i.e., $|A|\sim 0.001$ to ~ 0.1). Since it would seem highly improbable that *any* three quantities would satisfy relation (3.2), one is, therefore, led to conclude from the generally small magnitudes of the entries in Table IV, that the calculated values of the interaction potentials, both here and in II, are fairly reasonable.

It is of further interest to note that, for given Z_1 (chosen to be $<Z_2$ always), the average value of A, denoted by $\langle A\rangle$, increases monotonically with Z_2/Z_1 (see last two rows of Table IV). The same

TABLE III. Repulsive interaction energies $U(R)$ for heteronuclear rare-gas pairs not involving radon. DIR is direct calculation using Eq. (1.1). GM is computation using geometric-mean rule (1.4). R is the internuclear distance, r_{bi} $(i=1,2)$ the bounding radius of the ith TFD atom. (Atomic units are used throughout.)

$R(a_0)$	He-Ne		He-Ar		He-Kr		He-Xe		Ne-Ar	
	DIR	GM	DIR	GM	DIR	GM	DIR	GM	DIR	GM
0.01	1948	1949	3495	3497	6957	6963	10390	10410	17390	17390
0.03	615.7	617.2	1101	1102	2174	2180	3235	3241	5427	5427
0.06	287.7	284.0	510.0	510.7	998.9	1000	1477	1480	2485	2451
0.1	158.6	157.2	279.2	279.4	541.7	541.9	795.0	795.0	1340	1329
0.3	36.56	36.49	63.05	62.67	118.9	117.1	173.8	168.2	285.9	285.8
0.6	11.42	11.33	19.35	19.00	35.80	34.33	51.28	48.30	82.86	82.81
1.0	3.887	3.839	6.517	6.308	11.88	11.13	16.90	15.34	26.73	26.67
1.5	1.303	1.282	2.165	2.085	3.911	3.608	5.521	4.928	8.810	8.794
2.0	0.4763	0.4690	0.7898	0.7613	1.406	1.312	1.953	1.780	3.341	3.334
2.5	0.1712	0.1690	0.2842	0.2768	0.4986	0.4799	0.6815	0.6507	1.314	1.310
3.0	0.05928	0.05966	0.1001	0.1001	0.1770	0.1759	0.2414	0.2402	0.4982	0.4985
3.5	0.021[a]		0.034[a]		0.060[a]		0.084[a]		0.1730	0.1736
4.0	0.0078[a]		0.013[a]		0.022[a]		0.030[a]		0.06527	0.06448
4.5	0.0028[a]		0.0042[a]		0.0074[a]		0.010[a]		0.024[a]	
5.0	0.00097[a]		0.0016[a]		0.0026[a]		0.0037[a]		0.0091[a]	
5.5	0.00034[a]		0.00053[a]		0.00094[a]		0.0014[a]		0.0034[a]	
6.0	0.00013[a]		0.00019[a]		0.00033[a]		0.00048[a]		0.0013[a]	
r_{b1}	3.32100		3.32100		3.32100		3.32100		4.0507	
r_{b2}	4.05070		4.28180		4.52750		4.65770		4.2818	

$R(a_0)$	Ne-Kr		Ne-Xe		Ar-Kr		Ar-Xe		Kr-Xe	
	DIR	GM	DIR	GM	DIR	GM	DIR	GM	DIR	GM
0.01	34620	34620	51750	51770	62130	62130	92910	92910	184900	185000
0.03	10730	10730	15960	15960	19160	19170	28500	28500	56330	56370
0.06	4868	4802	7194	7102	8640	8636	12770	12770	25020	25020
0.1	2600	2577	3818	3780	4578	4579	6734	6717	13040	13030
0.3	537.6	534.1	773.8	767.1	919.5	917.3	1322	1318	2462	2462
0.6	151.9	149.6	215.5	210.5	252.5	250.8	356.8	352.9	638.3	637.7
1.0	47.98	47.07	67.33	64.85	77.52	77.33	108.8	106.5	188.6	188.1
1.5	15.64	15.22	21.79	20.79	24.93	24.75	34.59	33.80	58.64	58.51
2.0	5.891	5.747	8.175	7.796	9.392	9.329	12.97	12.66	21.91	21.81
2.5	2.314	2.270	3.181	3.080	3.745	3.721	5.145	5.045	8.763	8.748
3.0	0.8822	0.8760	1.207	1.196	1.472	1.470	2.025	2.007	3.532	3.527
3.5	0.3106	0.3128	0.4230	0.4320	0.5373	0.5385	0.7373	0.7437	1.321	1.340
4.0	0.1196	0.1156	0.1680	0.1607	0.1828	0.1829	0.2508	0.2542	0.4481	0.4558
4.5	0.045[a]		0.060[a]		0.080[a]		0.12[a]		0.1851	0.1830
5.0	0.018[a]		0.022[a]		0.030[a]		0.046[a]		0.066[a]	
5.5	0.0064[a]		0.0083[a]		0.012[a]		0.018[a]		0.026[a]	
6.0	0.0025[a]		0.0032[a]		0.0044[a]		0.0072[a]		0.010[a]	
r_{b1}	4.05070		4.05070		4.28180		4.28180		4.52750	
r_{b2}	4.52750		4.65770		4.52750		4.65770		4.65770	

[a] Extrapolated entries for $U(R)$.

holds very nearly even when Z_1 $(<Z_2)$ is not held fixed. This is probably to be explained as follows. According to the analysis given in I, the error made in calculating U_{TFD} via Eq. (1.1) increases monotonically as $Z_1 \to Z_2$. Hence, each of the values for U_{GM}, calculated with the aid of (1.4) and the results of II, wherein $Z_1=Z_2$ always, may be in error to the *maximum* extent of $\sim 4\%$ (as compared to the exact value in the TFD approximation).[19] In the direct calculation of U_{TFD} by means of (1.1), on the other hand, $Z_1 \neq Z_2$ invariably, and therefore the accuracy in U_{TFD} *thus* found should *increase* with Z_2/Z_1. Conse-

TABLE IV. Relative differences A, and their averages $\langle A \rangle$ (in %), between the present results and those obtainable from Ref. II by the geometric-mean rule (1.4).[a]

$R(a_0)$	He-Ne	He-Ar	He-Kr	He-Xe	Ne-Ar	Ne-Kr	Ne-Xe	Ar-Kr	Ar-Xe	Kr-Xe
0.01	0.052	0.058	0.087	0.19	···	···	0.039	···	···	0.054
0.03	0.15	0.091	0.28	0.19	···	···	···	0.052	···	0.071
0.06	−1.3	0.14	0.11	0.20	−1.4	−1.4	−1.3	−0.046	···	···
0.1	−0.89	0.072	0.037	···	−0.75	−0.89	−1.0	+0.022	−0.25	−0.077
0.3	−2.0	−0.61	−1.6	−3.2	−0.035	−0.65	−0.87	−0.22	−0.30	···
0.6	−0.79	−1.9	−4.2	−5.8	−0.061	−1.5	−2.3	−0.67	−1.1	−0.094
1.0	−1.3	−3.3	−6.4	−9.2	−0.23	−1.9	−3.7	−0.28	−2.1	−0.27
1.5	−1.7	−3.7	−7.8	−17	−0.19	−2.7	−4.6	−0.72	−2.3	−0.22
2.0	−1.6	−3.7	−6.7	−8.9	−0.21	−2.4	−4.6	−0.67	−2.4	−0.46
2.5	−1.3	−2.6	−3.8	−4.6	−0.31	−1.9	−3.2	−0.64	−1.9	−0.17
3.0	+0.65	···	−0.63	−0.50	+0.061	−0.70	−0.91	−0.14	−0.89	−0.14
3.5					0.35	+0.71	+2.1	−0.22	+0.87	+1.4
4.0					−1.2	−3.3	−4.3	−0.055	1.4	1.7
4.5										−1.1
$\langle A \rangle$	±1.1	±1.6	±2.9	±4.5	±0.37	±1.4	±2.2	±0.29	±1.0	±0.41
Z_2/Z_1	5	9	18	27	1.8	3.6	5.4	2	3	1.5

[a] Entries marked ··· refer to values smaller than 0.01%.

TABLE V. Repulsive interaction energies $U(R)$ for heteronuclear rare-gas pairs containing radon, calculated from Eq. (1.4) and the results of Ref. II. R is the internuclear distance; r_{bi} $(i=1,2)$ the bounding radius of the ith atom. (Atomic units are used throughout.)[a]

$R(a_0)$	He-Rn	Ne-Rn	Ar-Rn	Kr-Rn	Xe-Rn
0.01	16529	82191	147500	293680	439140
0.03	5110.7	25170	44942	88892	132180
0.06	2314.2	11108	19977	39140	57878
0.1	1234.3	5868.1	10428	20227	29666
0.3	253.00	1153.9	1982.2	3703.5	5318.9
0.6	70.701	308.21	516.51	933.43	1313.5
1.0	22.015	93.059	152.89	269.89	371.85
1.5	6.9719	29.410	47.822	82.780	113.05
2.0	2.5016	10.954	17.781	30.652	41.582
2.5	0.91473	4.3291	7.0919	12.298	16.675
3.0	0.33767	1.6815	2.8211	4.9578	6.7692
	.....				
3.5	0.12	0.61417	1.0575	1.9059	2.6318
4.0	0.043	0.23247	0.36764	0.65923	0.91658
		.....	.....		
4.5	0.016	0.091	0.17	0.24882	0.32092
				.....	.....
5.0	0.0056	0.034	0.063	0.098	0.13
5.5	0.00020	0.013	0.025	0.038	0.047
6.0	0.00075	0.0050	0.0095	0.014	0.018
r_{b1}	←		4.7952		→
r_{b2}	3.3210	4.0507	4.2818	4.5275	4.6577

[a] Entries below dotted lines are extrapolated.

quently, also the right-hand member of (3.1) should generally increase with Z_2/Z_1, as is indeed observed.

IV. INTERACTION POTENTIALS INVOLVING RADON

In contrast to the TFD curves given in Sec. II, those for systems of the type X-Rn (X=He, Ne, Ar, Kr, Xe) were calculated not directly from Eq. (1.1) but, instead, by the more expedient application of the GM rule (1.4) to the results obtained in II. Having just verified explicitly that this rule is generally well satisfied, it was felt that the determination of the X-Rn type potentials by this method [Eq. (1.4)] could be carried out with reasonable confidence. The numerical results of this part of the calculation are collected in Table V. A description of each of the five systems X-Rn follows.

A. Helium-Radon

For the He-Rn system (Fig. 15), no empirical data were available to the writer for judging the accuracy of U_{TFD}, and hence only the latter curve is shown here.

B. Neon-Radon

The Ne-Rn interaction is shown in Fig. 16. Only near the upper limit of $R(\sim 5.5a_0)$ are some empirical values[43] available for comparison with U_{TFD}. As is clear also from Table II, the agreement between U_{MB} and U_{TFD} near $R=5.5a_0$, is worst for this particular diatom (see also Sec. II A).

C. Argon-Radon

$R_l^{\mathrm{emp}} \simeq 6.2a_0$ for the Ar-Rn potential[43] (Fig. 17), and hence, only the criteria (2.3) and (2.4) are available for gauging the accuracy of U_{TFD} here. Down to $R\sim 1a_0$, both (2.3) and (2.4) are satisfied by U_{TFD}. In view of the wide latitude allowed by these conditions, however, all that can probably be deduced from this is that

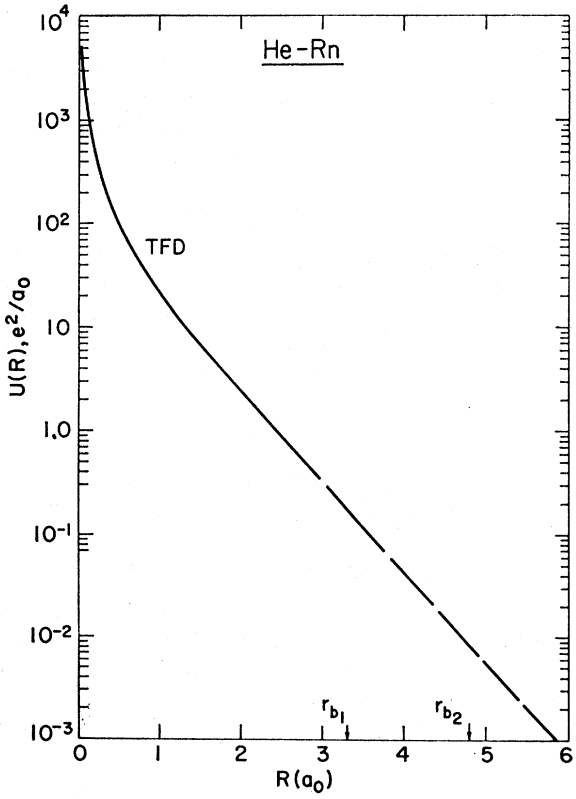

FIG. 15. Repulsive interaction potential for the He-Rn system.

[43] K. E. Grew and J. N. Mundy, Phys. Fluids 4, 1325 (1961).

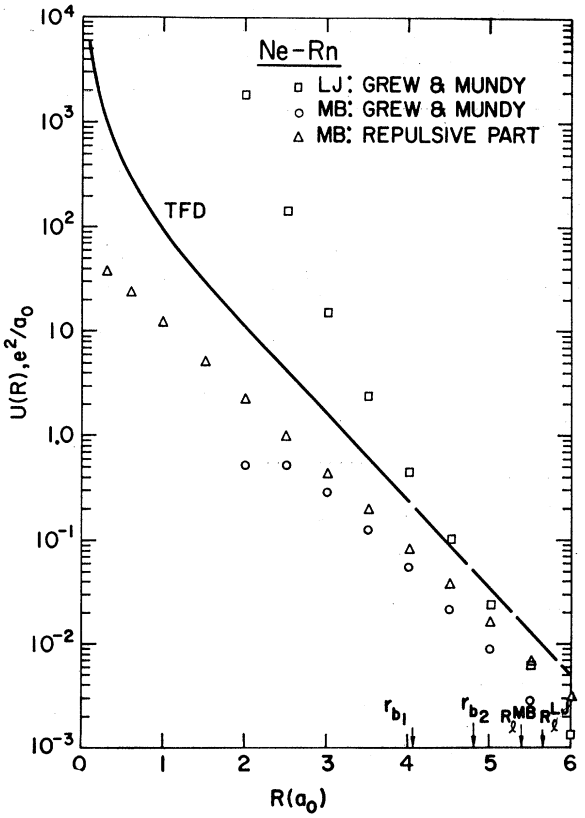

FIG. 16. Repulsive interaction potentials for the Ne-Rn system.

U_{TFD} for $1a_0 \lesssim R \lesssim 6a_0$ is unlikely to be in error by more than an order of magnitude. This state of affairs again emphasizes the great dearth of experimental data, especially on systems involving radon.

D. Krypton-Radon

For Kr-Rn (Fig. 18), $R_l^{\mathrm{MB}} \sim 6.3a_0$, and no (unextrapolated) empirical curves[43] suitable for comparison with U_{TFD} at $R < 6.0a_0$ could be found by the writer. Again, only conditions (2.3), (2.4) are, therefore, available for testing the TFD curve here (see also Sec. IV C).

E. Xenon-Radon

In the absence of other data on the Xe-Rn potential, only the results of this calculation are plotted in Fig. 19.

V. SUMMARY AND CONCLUSIONS

Application of the theoretical interaction potential (1.1) to the ten heteronuclear pairs of rare-gas atoms (exclusive of radon) studied here constitutes a detailed test of its actual reliability and, concomitantly, provides new and detailed information[44] concerning these interactions at internuclear separations R ranging, approximately, from 0.01 to $6a_0$. Similar information concerning the pairwise interactions involving radon has been obtained by application of the geometric-mean (GM) rule (1.4) to the results of Ref. II. Numerical values for U_{TFD} are generally calculable up to $R \simeq r_{b1}$ (where $r_{b1} < r_{b2}$ always), typically about 3–$4a_0$. For larger separations up to $R \sim 6a_0$, reasonable approximate values may be obtained by extrapolation. The TFD curves thus found have been compared, where feasible, with (a) empirical data; (b) other calculations; (c) the geometric-mean rule; (d) the appropriate united-atom energies. With regard to (a) and (b), this comparison supports the conclusions drawn from the study of the homonuclear pairwise interactions.[22] That is, the TFD curves (1) practically coincide with the Bohr potential at very small separations ($R \lesssim 0.1a_0$–$0.3a_0$) where U_{B} is generally considered to be reliable[6,8]; and (2) are in close or, at least, reasonable accord with the available empirical data in the approximate range $3a_0 \leq R \leq 6a_0$. In the intermediate range $0.3a_0 \lesssim R \lesssim 3.0a_0$, comparison of U_{TFD} was necessarily confined to that with mere extrapolations of the empirical curves. The agreement found here is comparable to that noted at the larger values of R, but, because of the extrapolations involved, the significance of the accord in this range must be viewed with reservation.

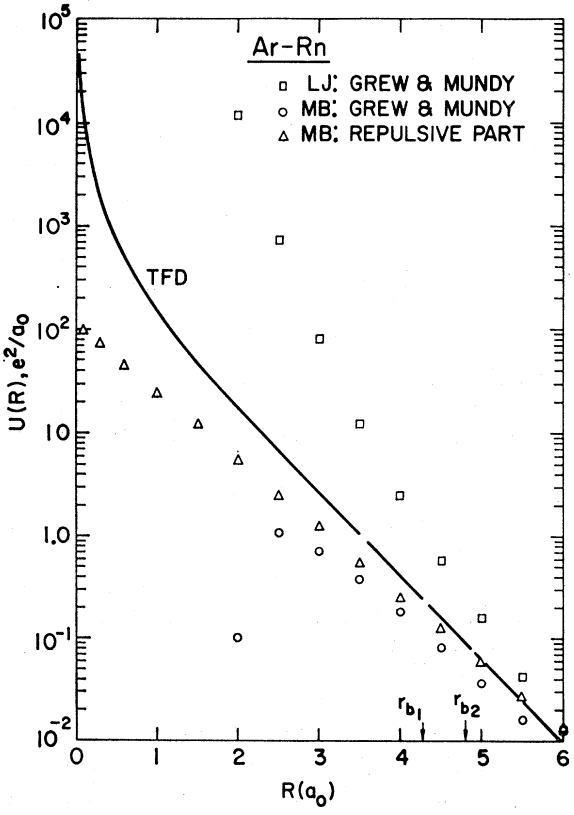

FIG. 17. Repulsive interaction potentials for the Ar-Rn system.

[44] Brief preliminary reports have been given in A. A. Abrahamson, Bull. Am. Phys. Soc. 7, 272 (1962).

For reasons not presently understood, agreement between U_{TFD} and experiment is generally worst for systems involving neon, and best for those containing argon. In each of the first ten systems here tested, on the other hand, the results of the present calculations agree more closely with experiment than does either Bohr's screened Coulomb potential[5] or Firsov's Thomas-Fermi-type potential.[45]

Relation (c) is found to be satisfied mostly to within $\sim 1\%$, thus giving added support to the validity of both the present results and those of II. As for (d), calculations for the He-Ne and Ar-Kr systems indicate that, as $R \rightarrow 0$, the electron energy of each system tends to the appropriate united-atom value (within the accuracy of the model).

In summary, then, one is led to conclude that at internuclear separations up to $\sim 6a_0$, the theoretical expression (1.1) (including its appropriate extrapolation), constitutes a reasonable representation of $U(R)$ and is generally considerably more accurate than are the Bohr or Firsov potentials wherever these differ from the TFD curve.

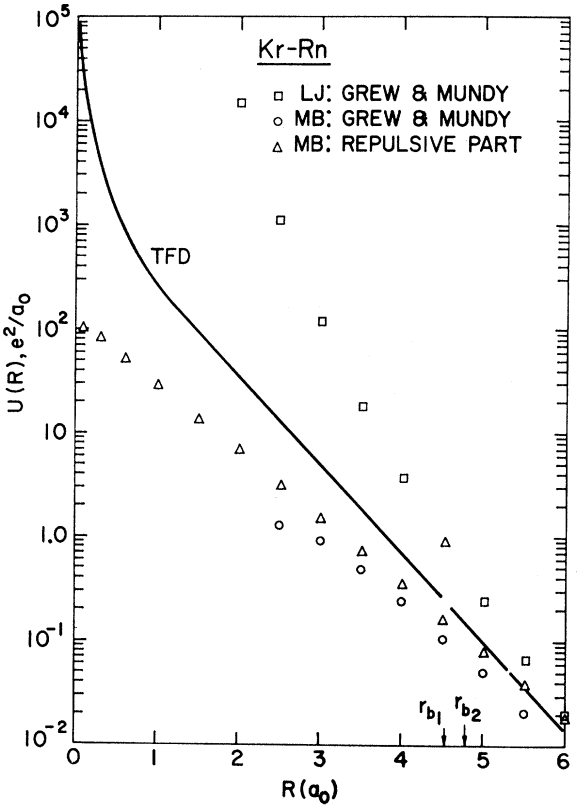

FIG. 18. Repulsive interaction potentials for the Kr-Rn system.

[45] While U_B and U_{TF} were not plotted for the five systems involving radon (Figs. 15–19), there appears to be no reason why U_B and U_{TF} should behave differently in these instances. The six cases studied in II further strengthen this conclusion.

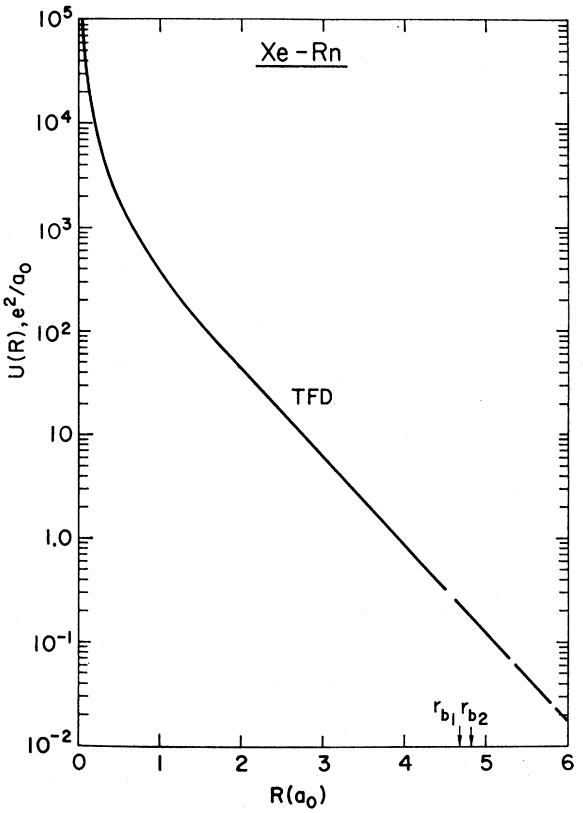

FIG. 19. Repulsive interaction potential for the Xe-Rn system.

In considering the conclusions here presented, it should be remembered, however, that these refer to only a restricted class of systems, characterized by *both* of the interacting atoms possessing closed-shell configurations. Inasmuch as the statistical model is applicable optimally to just such atoms,[21] the present conclusions concerning U_{TFD} may therefore have to be modified in the event that one or both members of an interacting pair of atoms have arbitrary shell configurations. Furthermore, for the latter kind of atoms, the failure of the present model to take the effects of correlation and inhomogeneity into account, may have more serious consequences.[34,46,47] Work on such systems, including other gases, metals, and certain diatoms, is in progress.[47]

ACKNOWLEDGMENT

The author wishes to express his gratitude to Dr. G. H. Vineyard for several stimulating discussions and helpful suggestions concerning this work.

APPENDIX

The calculation of the two-center integral $\bar{\Lambda}$ occurring in Eq. (1.1) and defined by (1.2) is prohibitively lengthy if done by hand, and hence was performed on a high-

[46] P. Gombas, Acta Phys. Acad. Sci. Hung. **9**, 451 (1959).
[47] A. A. Abrahamson, Bull. Am. Phys. Soc. **8**, 394 (1963).

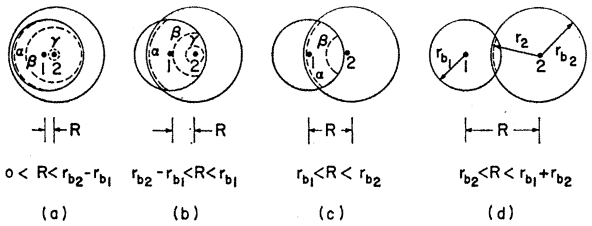

FIG. 20. Geometries, variables, and parameters used in the evaluation of the two-center integral $\bar{\Lambda}$ over the overlap region of a heteronuclear pair of TFD atoms, having respective radii r_{b1} and r_{b2}. The dashed arcs α, β, γ designate typical, distinct paths of integration for which r_2 is held constant while r_1 alone varies.

speed electronic computer. For the case of a homonuclear pair of TFD atoms, a method for computing $\bar{\Lambda}$ was described in II, and hence only the following modifications necessitated by the condition $Z_1 \neq Z_2$ are given here. Relations (A3) and (A4) of II become

$$\bar{\Lambda}=\frac{\pi}{3R}\int_{|R-r_2|}^{\min(r_{b1},R+r_2)} dr_1 \int_{\max(R-r_{b1},0)}^{\min(r_{b2},R+r_{b1})} dr_2\, r_1 r_2 F(r_1,r_2) \tag{A1}$$

and

$$r_{b1}<r_{b2}, \tag{A2}$$

respectively, with $F(r_1,r_2)$ denoting the integrand in $\bar{\Lambda}$. Expression (A1) can be shown to hold for arbitrary r_{bi} $(i=1,2)$, including the special case $r_{b1}=r_{b2}$, but otherwise subject only to the "ordering" prescribed by (A2). When $Z_1 \neq Z_2$, two cases can arise in principle:

$$r_{b2}>r_{b1}>\tfrac{1}{2}r_{b2} \tag{A3}$$

and

$$r_{b2}>r_{b1}\leq\tfrac{1}{2}r_{b2}, \tag{A4}$$

but in practice only (A3) is met, because the bounding radii of the smallest and largest TFD atoms of interest are $3.3210a_0$ and $4.8502a_0$ for helium and the element having $Z=105$, respectively.[48] That there are five distinct types of overlap consistent with (A2) and (A3) can best be seen from the upper row of diagrams in Fig. 2. Cases (a) to (c) there are new in the sense that these did not arise in II where $Z_1=Z_2$. Since $\bar{\Lambda}=0$ for zero overlap, i.e., when $R>(r_{b1}+r_{b2})$, only the first four cases depicted in Fig. 2 are redrawn in Fig. 20 (also showing typical, distinct paths of integration α, β, γ, on which $r_2=$ constant) in order to facilitate the determination of the limits of integration as follows: From Fig. 20(a) one readily finds that

$$0\leq r_2\leq R+r_{b1}, \tag{A5a'}$$

and that

$$\begin{aligned} &r_2-R\leq r_1\leq r_{b1} \quad \text{when} \quad r_{b1}-R<r_2<r_{b2} \text{ or path } \alpha \\ &r_2-R\leq r_1\leq R+r_2 \quad \text{when} \quad R<r_2<r_{b1} \text{ or path } \beta, \\ &R-r_2\leq r_1\leq R+r_2 \quad \text{when} \quad r_2<R \text{ or path } \gamma. \end{aligned} \tag{A5a}$$

Similarly, from Fig. 20(b),

$$0\leq r_2\leq r_{b2}, \tag{A5b'}$$

and

$$\begin{aligned} &r_2-R\leq r_1\leq r_{b1} \\ &\qquad \text{when} \quad R<r_2<R+r_{b1} \text{ or path } \alpha, \\ &R-r_2\leq r_1\leq r_{b1} \\ &\qquad \text{when} \quad r_{b1}-R<r_2<R \text{ or path } \beta, \\ &R-r_2\leq r_1\leq R+r_2 \quad \text{when} \quad r_2<r_{b1}-R \text{ or path } \gamma. \end{aligned} \tag{A5b}$$

From Fig. 20(c),

$$R-r_{b1}\leq r_2\leq r_{b2} \tag{A5c'}$$

and

$$\begin{aligned} &r_2-R\leq r_1\leq r_{b1}, \quad \text{when} \quad R<r_2<r_{b2} \text{ or path } \alpha, \\ &R-r_2\leq r_1\leq r_{b1}, \quad \text{when} \quad R-r_1<r_2<R \text{ or path } \beta. \end{aligned} \tag{A5c}$$

Finally, from Fig. 20(d),

$$R-r_{b1}\leq r_2\leq r_{b2},$$

and

$$R-r_2\leq r_1\leq r_{b1}. \tag{A5d}$$

Despite the multiform appearance of these limits, it is not difficult to show that all four sets of relations (A5) can be combined into the single set

$$\begin{aligned} &\max(R-r_{b1},0)\leq r_2\leq \min(r_{b2},R+r_{b1}) \\ &\qquad |R-r_2|\leq r_1\leq \min(r_{b1},R+r_2) \end{aligned} \tag{A6}$$

valid for each and all of the four cases shown in Fig. 20, and therefore appropriate as indicated in (A1).

[48] L. H. Thomas, J. Chem. Phys. 22, 1758 (1954).